Representational structure of fMRI/EEG responses to dynamic facial expressions

Muukkonen, Ilkka

2022-11

Muukkonen , I & Salmela , V 2022 , ' Representational structure of fMRI/EEG responses to dynamic facial expressions ' , NeuroImage , vol. 263 , 119631 . https://doi.org/10.1016/j.neuroimage.2022.119631

http://hdl.handle.net/10138/349921
https://doi.org/10.1016/j.neuroimage.2022.119631

NeuroImage 263 (2022) 119631

Contents lists available at ScienceDirect

NeuroImage

journal homepage: www.elsevier.com/locate/neuroimage

Representational structure of fMRI/EEG responses to dynamic facial expressions

I. Muukkonen, V.R. Salmela*

Department of Psychology and Logopedics, University of Helsinki, Finland

ARTICLE INFO

Keywords:
EEG
fMRI
RSA
Facial expression
Decoding
Face perception
Dynamic faces

ABSTRACT

Face perception provides an excellent example of how the brain processes nuanced visual differences and transforms them into behaviourally useful representations of identities and emotional expressions. While a body of literature has looked into the spatial and temporal neural processing of facial expressions, few studies have used a dimensionally varying set of stimuli containing subtle perceptual changes. In the current study, we used 48 short videos varying dimensionally in their intensity and category (happy, angry, surprised) of expression. We measured both fMRI and EEG responses to these video clips and compared the neural response patterns to the predictions of models based on image features and models derived from behavioural ratings of the stimuli. In fMRI, the inferior frontal gyrus face area (IFG-FA) carried information related only to the intensity of the expression, independent of image-based models. The superior temporal sulcus (STS), inferior temporal (IT) and lateral occipital (LO) areas contained information about both expression category and intensity. In the EEG, the coding of expression category and low-level image features were most pronounced at around 400 ms. The expression intensity model did not, however, correlate significantly at any EEG timepoint. Our results show a specific role for IFG-FA in the coding of expressions and suggest that it contains image and category invariant representations of expression intensity.

1. Introduction

A person's face often provides the best visual cues when we recognize someone, or want to know how they feel or what they are thinking. Relatively small movements of the eyes or mouth can be enough to indicate whether someone is filled with joy or overwhelmed by fear. The ease with which our brain achieves this feat has prompted the idea that we are experts in face recognition (e.g., Kanwisher, 2000; Rossion, 2018). One of the main research questions has been how the brain transforms visual facial features into representations of identities and emotional states. The encoding of expressions and identities likely differs, since while the end goal of identity coding is usually a categorical decision of "is/isn't person X", expressions also contain a dimensional aspect. Although it is important for the perceiver to notice whether someone is happy or angry, the intensity of the emotion provides crucial information as well. In this study, we investigated brain processes related to the perception of subtle changes in expression intensity.

There is a considerable body of literature investigating the areas and timing of face processing in the brain (for reviews, see e.g., Duchaine & Yovel, 2015; Kovács, 2020). Based mainly on fMRI studies and single-cell studies on monkeys (e.g., Chang & Tsao, 2017; Eifuku, 2014; Freiwald & Tsao, 2010; Freiwald, Tsao, & Livingstone, 2009; Leopold, Bondar, & Giese, 2006; Perrett, Rolls, & Caan, 1982; Sugase, Yamane, Ueno, & Kawano, 1999; Yang & Freiwald, 2021), several areas involved in face perception have been proposed, most notably including the fusiform face area (the FFA; Anzellotti, Fairhall, & Caramazza, 2014; Carlin & Kriegeskorte, 2017; Dobs, Schultz, Bülthoff, & Gardner, 2018; Kanwisher & Yovel, 2006) in the fusiform gyrus, the occipital face area (the OFA; Atkinson & Adolphs, 2011; Henriksson, Mur, & Kriegeskorte, 2015; Pitcher, Walsh, & Duchaine, 2011) in the lateral occipital (LO) area, the superior temporal sulcus (the STS; Greening, Mitchell, & Smith, 2018; Said, Haxby, & Todorov, 2011; Zhang et al., 2016), the anterior temporal lobe (the ATL; Anzellotti & Caramazza, 2016; Anzellotti et al., 2014; Collins & Olson, 2015; Kriegeskorte, Formisano, Sorger, & Goebel, 2007), and the inferior frontal gyrus face area (the IFG-FA; Chan & Downing, 2011; Engell & Haxby, 2007; Flack et al., 2015). The roles of the different areas have been roughly divided between a ventral path (especially the FFA and ATL) involved more in the stable features of a face, used to identify a person, and a dorsal path (the STS) for the processing of moving face parts and facial expressions (Duchaine & Yovel, 2015). The processing of identity is thought to start from the low-level, non-face-specific visual feature coding in the early visual cortex (the EVC), reaching to the OFA for the coding of face parts, to the FFA for a somewhat image-invariant

* Corresponding author.
E-mail address: viljami.salmela@helsinki.fi (V.R. Salmela).

https://doi.org/10.1016/j.neuroimage.2022.119631.
Received 22 December 2021; Received in revised form 9 September 2022; Accepted 12 September 2022
Available online 13 September 2022.

representation of a face identity, and to the ATL and other more frontal areas for the final representation of a person's identity (Duchaine & Yovel, 2015).

The M/EEG studies show at least four important timings for face processing: 100 ms, 170 ms (the N170 component), early positive negativity (EPN) around 170–350 ms, and 400 ms. The processing of low-level visual features of faces, and also perhaps some identity and expression representations (Ambrus, Kaiser, Cichy, & Kovács, 2019; Dima, Perry, Messaritaki, Zhang, & Singh, 2018; Dobs, Isik, Pantazis, & Kanwisher, 2019; Dzhelyova, Jacques, & Rossion, 2017; Leleu et al., 2018; Müller-Bardorff et al., 2018)(Smith & Smith, 2019), has been shown in multiple studies to start around 100 ms after stimulus onset (Dima et al., 2018; Muukkonen, Ölander, Numminen, & Salmela, 2020; Smith & Smith, 2019; Sugase et al., 1999). The N170 component at 170 ms after stimulus onset (for a review, see Rossion & Jacques, 2011) is already sensitive to some expression categories and intensity (Hinojosa, Mercado, & Carretié, 2015; Recio, Schacht, & Sommer, 2014), as is the subsequent EPN after 200 ms (Leppänen, Kauppinen, Peltola, & Hietanen, 2007; Recio et al., 2014; Sprengelmeyer & Jentzsch, 2006). Facial motion (moving eyes/mouth) compared to static images or non-facial motion modulates the latency and amplitude of responses around 170 ms (Puce, Smith, & Allison, 2000; Watanabe, Kakigi, & Puce, 2001). Finally, around 400 ms, image-invariant representations of face identities emerge (Ambrus et al., 2019; see also Smith & Smith, 2019). When comparing different expressions, studies have found differences to be most pronounced when comparing neutral or fearful expressions with other expressions (Poncet, Baudouin, Dzhelyova, Rossion, & Leleu, 2019), and the differences between fearful and neutral after 200 ms (Leppänen et al., 2007). A few studies have been conducted on the intensity of expressions, finding that the processing of intensity started as early as 100 ms (Leleu et al., 2018) and more pronounced signal negativity from N170 onwards (Sprengelmeyer & Jentzsch, 2006). Dynamic faces compared to static faces evoke more widespread activity in temporal and frontal regions, both in early and late time windows (Recio, Sommer, & Schacht, 2011; Trautmann-Lengsfeld, Dominguez-Borras, Escera, Herrmann, & Fehr, 2013). Most of the EEG studies have used univariate methods, but MVPA has been used in some studies of face identities (Ambrus et al., 2019; Dobs et al., 2019; Smith & Smith, 2019) and expressions (Muukkonen et al., 2020; Smith & Smith, 2019).

In the dorsal face path, namely the STS and IFG-FA, a common finding is the enhanced response to dynamic compared to static faces (e.g., Foley, Rippon, Thai, Longe, & Senior, 2012; Fox, Moon, Iaria, & Barton, 2009; Furl et al., 2010; Pitcher, Dilks, Saxe, Triantafyllou, & Kanwisher, 2011; Pitcher, Duchaine, & Walsh, 2014; Trautmann, Fehr, & Herrmann, 2009; Yoshikawa & Sato, 2006) and the enhanced response to facial motion compared to other types of visual motion (Furl et al., 2010; Puce et al., 2003; Sato, Kochiyama, & Uono, 2015), leading to the suggestion that the main function of the dorsal path is the processing of facial motion (Bernstein & Yovel, 2015). Recent studies have shown the STS to contain part-based code of subtle movements of eyes and mouth (Deen & Saxe, 2019), both the STS and IFG-FA to respond more to asynchronous than synchronous face movements (Skiba & Vuilleumier, 2020), and the STS to contain code of the movements of facial action units (Srinivasan, Golomb, & Martinez, 2016). For facial expressions, the STS has been shown, for example, to integrate vocal emotions and facial expressions (Watson et al., 2014), to manifest release from adaptation for changing expressions but also for identities (Fox et al., 2009), and to display higher responses to higher expression intensities (Winston, O'Doherty, & Dolan, 2003). However, some of the studies that indicated motion coding in the STS or IFG found only weak (Srinivasan et al., 2016) or no (Foley et al., 2012) differences between expression categories in the STS, and coding of expression intensity in the STS but not in the IFG (Skiba & Vuilleumier, 2020). For more detailed expression coding, perceptual similarity of different expressions was shown to correlate with the STS (Sormaz, Watson, Smith, Young, & Andrews, 2016), and the STS to contain continuous representation of the intensity of the expression (Harris, Young, & Andrews, 2012), in contrast to the amygdala having categorical representations (Harris et al., 2012; Harris, Young, & Andrews, 2014). The evidence for the role of the IFG in facial expression coding is sparser, with studies showing higher activation towards expressive rather than neutral faces (Engell & Haxby, 2007), processing of the eyes in particular (Chan & Downing, 2011), and one study showing it to contain more holistic representations of emotional faces than the STS (Flack et al., 2015). One challenge for finding brain regions sensitive to expression coding is to separate it from motion processing (Bernstein & Yovel, 2015).

In the current study, we looked at the spatial (with fMRI) and temporal (with EEG) neural responses to the category and intensity of facial expressions (Fig. 1). Our aim was to dissociate expression intensity coding from facial motion processing and the processing of expression categories. We showed participants short video clips that varied dimensionally in small steps from neutral to intense, and between happy, angry, and surprised. Thus, all of our stimuli contained a similar type of facial motion, but one half contained changes in expression intensity and the other half changes in expression category. With multivariate-pattern analysis (MVPA) and representational similarity analysis (RSA), we compared the data from the EEG and fMRI to image-based models (Gabor filter, block motion, mean contrast, and OpenFace face processing algorithm) and behavioral models of the observed level of expression intensity, happiness, surprise, angriness, and expression category of each stimulus. This allowed us to look for the more precise neural codes for different aspects of facial expressions in different brain regions and at different times. Compared with previous studies, we used a relatively large set of stimuli (48), strictly controlled several (low-level) features of the faces, and applied the MVPA to distinguish more fine-grained neural responses. Our results shed light on the spatial locations of facial expressions, highlighting the coding of expression intensity, independent of low-level features or expression category, in the IFG-FA, while the STS, LO and IT coded both intensity and category of expressions. In the EEG, we found two main peaks at 150 ms and 400 ms, both related to low-level visual features and the processing of expression categories with no evidence of expression intensity coding.

2. Methods

2.1. Participants

Twenty participants (14 female) were recruited to the study (including the two authors) from the student mailing lists of the University of Helsinki. The sample size was determined by previous studies using similar methods. The mean age of the participants was 29 (range 19–46). Participants were screened (by self-report) to have normal or corrected to normal vision, to have no diagnosed difficulties in face perception (e.g., prosopagnosia), to be 18–50 years old, to have no diagnosed neurological issues, and to be suitable for MRI measurement (to have no metal in the body). In addition, due to the Covid-19 situation during the measurements, special safety protocols of Aalto University and the University of Helsinki were followed. Specifically, the participants were also screened not to belong to any Covid-19 risk group, not to have any symptoms before the measurement days, and not to have travelled abroad two weeks prior to the measurements. In the event of any symptoms, the measurements were rescheduled. Participants received monetary compensation (€15/h) for their participation.

2.2. Ethics

The present study was conducted in accordance with the Declaration of Helsinki, and was reviewed and approved by the Ethics Review Board in the Humanities and Social and Behavioral Sciences of the University of Helsinki. All participants gave informed consent and were screened for suitability for fMRI scanning, adhering to the standard procedure of the AMI Centre at Aalto University.

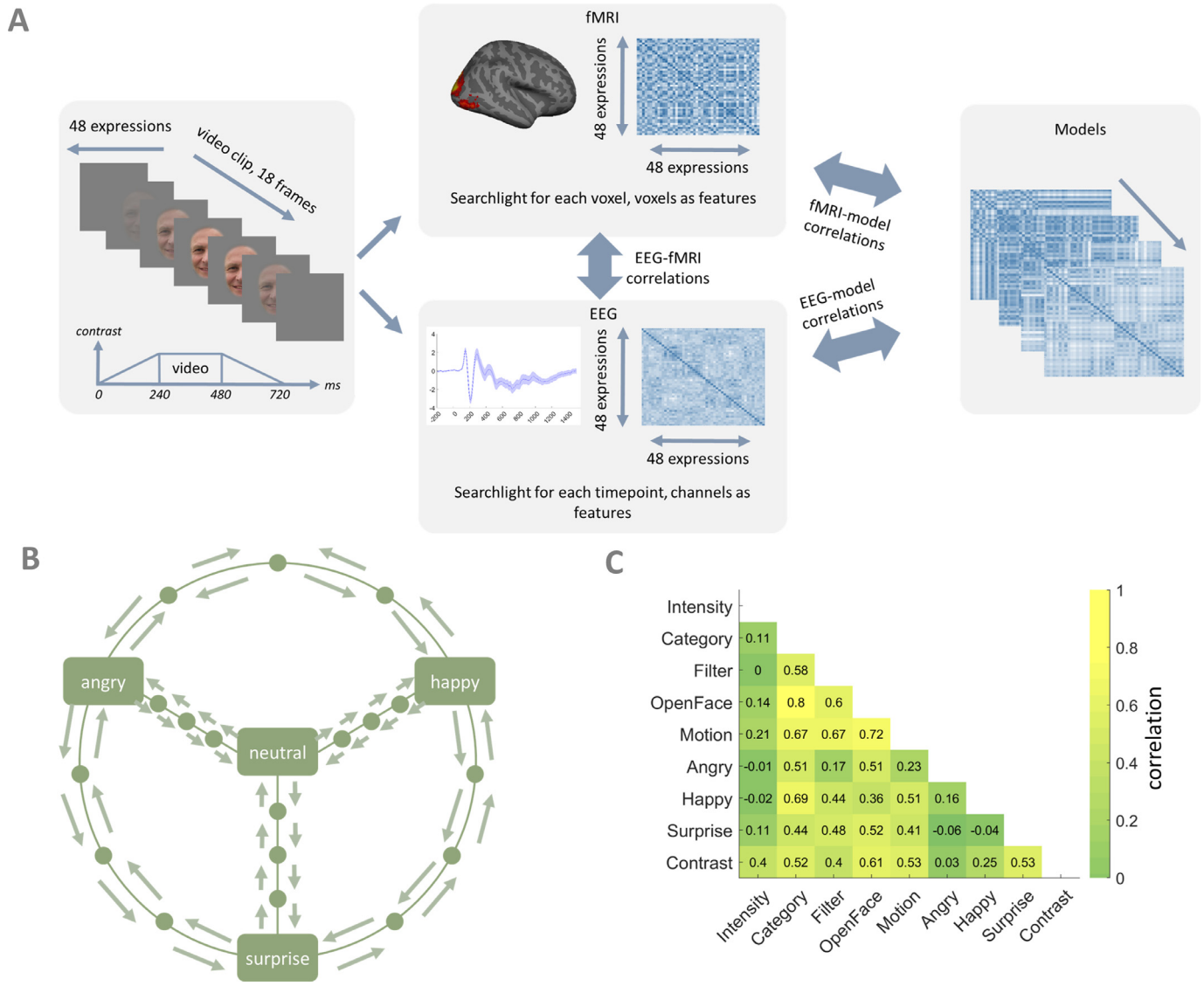

Fig. 1. Study design, stimuli space, and correlations between models. **A)** Study design. Left: each trial contained a short video clip of a facial expression. Middle: both fMRI and EEG responses to the same stimuli were measured (in separate sessions), and RDMs were calculated for each voxel in the fMRI with a searchlight, and for each timepoint in the EEG. Right: these RDMs were then correlated to each other, and to different models. **B)** Schematic stimulus space. Each arrow represents one stimulus (48 in total). We morphed three expressions and neutral faces into each other, taken from 12 identities. Each stimulus was a short video clip from the morph continuum, divided in four parts of equal length. **C)** Correlations between models.

2.3. Stimuli

Our stimuli comprised 48 short video clips of facial expressions, varying in their intensity or expression category (Fig. 1). We used three different expressions (happy, angry, surprised), which were morphed between themselves, as well as between each expression and a neutral face. The video clips were constructed from the morphs. As depicted in Fig. 1B, we used 4 morph levels with equal steps. On a morph continuum from 1 (e.g., angry) to 100 (e.g., happy), the video clips were from 1 to 25, from 26 to 50, from 51 to 75, and from 76 to 100, in both directions. Thus, there were 3 expression-to-expression continuums (angry-happy, angry-surprised, happy-surprised), with 4 levels and 2 directions, resulting in 3×4×2 = 24 stimuli, varying between expressions, and 3 neutral-to-expression (neutral-angry, neutral-happy, neutral-surprised) continuums, with 4 levels and 2 directions, also resulting in 24 stimuli, varying between expression and neutral face. In addition, to reduce the role of image- and identity-specific features, we created these 48 expression videos for 12 different identities.

All face images were taken from the Radboud Faces Database (Langner et al., 2010), aligned based on the position of the eyes, and resized to be approximately the same size to improve the results of the morphing, as well as to limit low-level visual variation between the images. Each video contained 18 frames and the length of the clips was 720 ms (Fig. 1A). In the first/last 6 frames, the contrast of the face was linearly faded in/out. In the middle frames 7–12, the expression changed with 6 different morph steps. Thus, the duration of expression change was 240 ms (240–480 ms from stimulus onset). The size of the stimuli were slightly different in the fMRI and EEG experiments. In the fMRI experiment, the faces were 570×800 pixels in size (10×14 cm), corresponding 14.3×19.9 degrees of visual angle (with a viewing distance of 40 cm). In the EEG experiment, the faces were 660×920 pixels in size (18×25 cm), corresponding 12.8×17.8 degrees of visual angle (with a viewing distance of 80 cm). The RMS contrast of the stimulus was 0.19+/-.02. The expression categories were selected to contain one expression with positive valence (happy), one with negative valence (angry), and one with relatively neutral valence (surprised).

2.4. General study design

The experiment comprised three main parts: fMRI measurements, EEG measurement, and behavioral ratings. These were conducted on three separate days, with two days involving fMRI measurement and one day EEG measurement. In addition, on each day, behavioral ratings of the stimuli were collected either before or after the EEG/fMRI. Nine participants conducted the EEG session first, and eleven participants the fMRI sessions first. The gap between the sessions for each participant varied from 5 to 40 days, and between the two fMRI sessions from 3 to 29 days (mean 11.3 days).

The procedures were almost the same in the EEG and fMRI, and any exceptions are noted further below. The participants were shown short video clips of expressions, and were instructed to concentrate on watching the videos, focusing their gaze on a cross in the middle of the screen (the fixation cross was visible during the whole experiment), and to perform one of the following two tasks. In the *1-back task*, a video clip was repeated twice in a row, and participants were instructed to press a button every time they saw a repeated video clip. In the *oddball task*, the facial expression in the target video clips changed direction in the middle of the video instead of continuing to move only in one direction (as in all non-target clips). Again, participants were instructed to press a button when they noticed a video with this odd movement. These tasks alternated between runs. The tasks were selected to ensure that participants' attention would be drawn to the whole face for the duration of the video. We used two tasks instead of one in order to find results that would generalize across tasks, and be independent of a specific task.

There were 12 runs in the EEG (recorded in one session) and 12 in the fMRI (recorded in two six-run sessions). Each run included each of the stimuli twice (96 main trials in total), firstly showing each stimuli once in random order, and then each for the second time in random order. In the fMRI, there was a 30-second rest period in the middle of the run. The inter-stimulus-interval (ISI) was 1-1.5 seconds in the EEG and 2-2.5 seconds in the fMRI, containing (uniformly distributed) random 0-500 ms jitter. In addition, there were 10 target trials in each run (see above), occurring randomly with restrictions of no two targets in a row, and no target being the first trial of a run or after the rest period. Participants were contacted via microphone between each run and were allowed to rest if needed. In addition, as all 12 EEG runs were conducted in one long session, a longer rest was taken approximately halfway through the session. During this longer rest period, the participants were offered light refreshments. The quality of the EEG data was observed online, and the electrodes were adjusted in the few cases where there was a drop in the data quality in some channels (impedance<60kOhm).

Finally, a behavioral rating task was conducted in each session. In the EEG session, the participants completed the rating task before the main experiment during the preparation of the EEG cap. In the fMRI sessions, the rating was usually performed after the main experiment with a couple of exceptions. In the rating task, the same video clips were shown as in the main experiments. The video clip was running repeatedly on the left side of the screen, and participants were instructed to rate it on four different qualities: how happy, angry, surprised, and emotionally intense the face appeared. The ratings were conducted with sliders, which were adjusted using a mouse. All of the sliders were shown at the same time on the right side of the screen, and participants could adjust them any way they pleased, after which they pressed a button which started a new trial with a new video clip. The sliders used a scale from 0 to 100 and were set at 50 at the beginning of each trial. In each session, each participant rated each of the 48 videos twice, with 96 ratings per session, and 288 for each participant in total. The identity of the face in each video clip was randomized in all EEG, fMRI, and rating experiments. The order of videos in each run was random for each participant, but due to a minor bug in the experiment script, the same random order was used for several participants.

2.5. Functional localizers and ROIs

The face-selective regions were mapped with two functional localizers, one containing video clips of faces and moving objects, and the other containing still images of faces and objects. The results of these localizers were not, however, used in any of the analyses and are therefore not reported in more detail.

2.6. EEG acquisition and preprocessing

The EEG data were recorded with a 64-channel cap (actiCHamp, Brain Products) and active electrodes in a shielded room and sampled online at 1024 Hz. Preprocessing was performed with EEGLAB v13.5.4b running in MATLAB R2019a, separately for each participant. We downsampled the data to 250Hz, applied a band-pass filter between 0.05 and 40 Hz, rejected noisy channels (using a 'pop_rejchan' EEGLAB function with default parameters) and interpolated (spherical) them back into the data. We then epoched the data for independent component analysis (ICA) between -500 and 1500 ms related to the stimulus onset, ran the ICA (fastica; Hyvärinen, 1999), removed bad ICA components with the 'interface_ADJ' (Mognon, Jovicich, Bruzzone, & Buiatti, 2011) automated component selector algorithm (for one participant no ICA components were removed), created epochs from -200 to 1500 ms related to stimulus onset, removed the baseline, and sorted the trials into the 48 different stimuli types. No trials were removed, and each participant had 24 trials per stimuli type. This all resulted in the EEG dataset of 20 participants x 63 channels x 48 stimuli type x 425 timepoints (4 ms each).

2.7. fMRI acquisition and preprocessing

Functional MRI data were recorded using a 3T MAGNETOM Skyra scanner (Siemens Healthcare, Erlangen, Germany) at the AMI Centre of Aalto University School of Science. Each participant completed two fMRI sessions on two different days. A 30-channel head coil was used. Blood-oxygen level dependent (BOLD) signals were acquired with a simultaneous multislice (SMS; multiband factor 4) echo-planar imaging (EPI) sequence. The imaging area consisted of 76 oblique slices with 2.0×2.0 mm voxels (slice thickness 2.0 mm, interslice gap 0 mm), TR was 2.08 s (except for the first participant's first session, when TR was 2.1s), TE was 34 ms, flip angle was 75, matrix size was 100×100, and the field of view was 200. Both fMRI sessions started with an anatomical T1 scan (MPRAGE), lasting approximately 6 minutes, followed by a *face video localizer* run (7 mins, 200 volumes). After that, six experimental runs were performed (6 min, 175 volumes each). Finally, and only in the first session, a *face image localizer* run (7.5 mins, 210 volumes) was measured.

The fMRI data were preprocessed using fMRIPrep 20.1.1 (Esteban, Markiewicz, et al. 2018; Esteban, Blair, et al. 2018). Please see the Supplementary Material for detailed information on preprocessing.

The fMRI data were modelled with an event-related GLM analysis containing separate regressors for each stimulus type (48 in total), and 37 nuisance regressors. The nuisance regressors were target stimulus, global signal, framewise displacement, 6 motion parameters, 4 cosine components, and 24 first compCorr components. As a result, there were 48 (stimuli) x 12 (runs) whole-brain beta images for each participant for the subsequent analyses.

2.8. Behavioral and image-based models

We created five *behavioral models* based on the ratings of the stimuli in the rating task, one for *Intensity*, one for each expression category (*Angry, Happy, Surprised*), and a combined model for the expression categories (*Category*). First, the multiple ratings for the same stimuli type (irrespective of the face identity) and the same rating quality (*angry,*

happy, surprised, or emotion *intensity*) were averaged separately for each participant. Then, an RDM was created based on the distances between the rating of each possible stimulus pair. Thus, we had one RDM for each of the qualities for each participant. These RDMs were then averaged across participants to create the final behavioral models. For the combined *Category* model, we took the point distances between each stimuli in the three-dimensional space of the three expression categories.

The four *image-based* models included a spatial Gabor *Filter* model, a block *Motion* model, a model for mean *Contrast*, and the *OpenFace* model. The *Filter* model was created by first computing the Gabor filter outputs for the last high-contrast frame of the videos (with the ComputeStaticGabors function; https://github.com/gallantlab/; Nishimoto, Vu, Naselaris, Benjamini, Yu, & Gallant, 2011), and by correlating the filter outputs across stimuli and subtracting the correlation matrix from one. The *Motion* model was created by first calculating the block motion between frames (with MATLAB's BlockMatcher function using a block size of 9×9 pixels), and then correlating motion estimates across stimuli and subtracting the correlation matrix from one. The *Contrast* model was computed based on the differences in mean rms contrast between the last high-contrast frame of the videos. Note that the contrast variation between stimuli was very modest, only mean+/-2% point. The *OpenFace* model was calculated based on the OpenFace algorithm (https://cmusatyalab.github.io/openface/; Amos, Ludwiczuk, & Satyanarayanan, 2016), which is trained to separate different face identities from each other. Thus, it is not explicitly meant to differentiate between facial expressions. The algorithm provides a differentiation score between each face image pair, and we used these scores to create the model. Thus, we used a total of five behavioural models (*Happy, Angry, Surprised, Intensity, Category*) and four image-based models (*Filter, Motion, Contrast, OpenFace*). The correlations between the models are shown in Fig. 1 C and were all between .10 and .70.

2.9. EEG model, fMRI model and EEG-fMRI correlations

We tested where and when the different models correlated with neural data with a representational similarity analysis (RSA; Kriegeskorte, Mur, & Bandettini, 2008). In the EEG, an RDM was created separately for each timepoint and for each participant by calculating the 1-correlation (Pearson) of the 63 EEG channels at a given time between each possible stimulus pairs. Each cell in the RDM is thus a score of the dissimilarity between the stimulus *y* and *x*. Similarly, in fMRI, an RDM was calculated for each voxel. This was performed using a moving searchlight (Kriegeskorte, Goebel, & Bandettini, 2006) with an 8mm radius, in which all voxels within the radius of a given voxel are used to form one vector for each stimulus type. The 1-correlation (Pearson) between each possible stimulus pair was again used as the distance metric. We used mean pattern normalization in both EEG and fMRI by normalizing the response (i.e., subtracting the mean and dividing with the standard deviation) of each channel and each timepoint in the EEG and each voxel in the fMRI to all of the stimulus types, and all z-values higher/lower than +-3 were set as +-3. Finally, these RDMs from each participant were correlated (Spearman) with the model RDMs (see above), and this resulted in a time course (in the EEG) or a spatial map (in the fMRI) for each of the models. We report the results from correlations and partial correlations, controlling for the role of all of the other models. For the EEG-fMRI correlation, the RDMs from each fMRI voxel and each EEG timepoint were correlated to create a four-dimensional spatio-temporal map. The EEG data (but not the fMRI data) were averaged across participants before the correlation.

2.10. Statistical analyses

All statistical inferences were derived from permutation analyses (Nichols & Holmes, 2001). Namely, we shuffled the signs of the participants' correlations 5,000 times, and for each permutation, the same analysis was conducted as for the real data. This resulted in an empirically derived distribution of statistics under the null hypothesis, and statistical significance was taken as the top 5% of the permuted statistics for one-tailed significance tests ($p<.05$). For the fMRI model correlations, we used the SnPM toolbox for SPM, and variance smoothing (6 mm) as suggested in Nichols and Holmes (2001), with a cluster-forming voxel threshold of $T = 3$ ($P=.004$), and cluster-size inference ($p<.05$). In the EEG-model correlations, we used an in-house script to calculate the permutations, with a cluster-forming threshold of $p<.05$, and a cluster-mass inference (based on the sum of the cluster's t-values). The thresholds and inference methods were chosen for consistency to be the same as in our previous similar study (Muukkonen et al., 2020). No family-wise error correction across models was used. In the EEG-fMRI, we calculated four-dimensional clusters (with the 'bwconncomp' function in MATLAB), with a cluster-forming threshold of $T = 3$ and a cluster size inference.

There were three main modifications to our planned analyses, namely a change from using support vector machines (SVM) first to cross-validated Mahalanobis distance ('crossnobis'; Walther et al., 2016), and then to simple correlation (not cross-validated), and adding the use of a mean-pattern reduction (MPR). Thus, we report all our results with a Bonferroni-corrected $p<.05$ for four tests (raw p-value of $<.0125$). The Bonferroni-correction was applied to the final p-values. As cross-validated methods are usually preferred (Walther et al., 2016; but see Ritchie, Lee Masson, Bracci, & Op de Beeck, 2021), SVM and crossnobis were our preliminary options. Unexpectedly, the SVM showed very weak or non-existent results for both the EEG and fMRI. For crossnobis and correlation analysis, while the EEG results were very similar between the methods, we saw practically no fMRI-model correlations with crossnobis outside of the early visual cortex. In contrast, the correlation metric with mean-pattern normalization showed quite pronounced and sensical model correlations in many face areas. Furthermore, we first used correlation analyses without mean-pattern normalization (similar to mean-pattern reduction; MPR) and implemented it post-hoc (see Walther et al., 2016 for the effect of mean pattern reduction on the RDMs). Thus, we report the results from the MPR correlations, while the results from the crossnobis analyses and correlation analyses without mean-pattern normalization can be found in the Supplementary Material, and further remarks on this selection in the Discussion section.

3. Results

3.1. Behavioral results

In the EEG and fMRI measurements, we used two attention control tasks, oddball and 1-back. The mean hit rates for the two tasks were 83.3% and 88.1% in the EEG, and 70.8% and 87.2% in the fMRI, showing that all participants had focused their attention on the stimuli. In the behavioural rating task, participants agreed on ratings quite well and the mean correlations (SDs) between different participants' ratings for intensity, angry, happy and surprised were .64 (.11), .71 (.08), .77 (.08), and .68 (.11), respectively. The correlations between rating sessions (3 sessions, each stimuli shown twice with random identity per session) within subjects were .51 (.17), .66 (.14), .77 (.08), and .64 (.15), respectively. Differences between the within-subject reliability of the different expression ratings were significant (t-test, all $p <.01$), except between the angry and surprise ratings ($p=.52$).

We created RDMs based on the morph-level of the stimuli to test whether the behavioural ratings corresponded to the 'true' morph-levels. The morph distance between stimuli is shown in Fig. 1B. For example, all the morphs between expressions (arrows on the ring in Fig. 1) were given maximum value for morph Intensity model, and the morphs between neutral face and expressive face are given values based on their distance of the neutral (closest to neutral = minimum intensity). The expression morph models were created similarly. Table 1 shows the correlations between these morph-based models and the behavioral models.

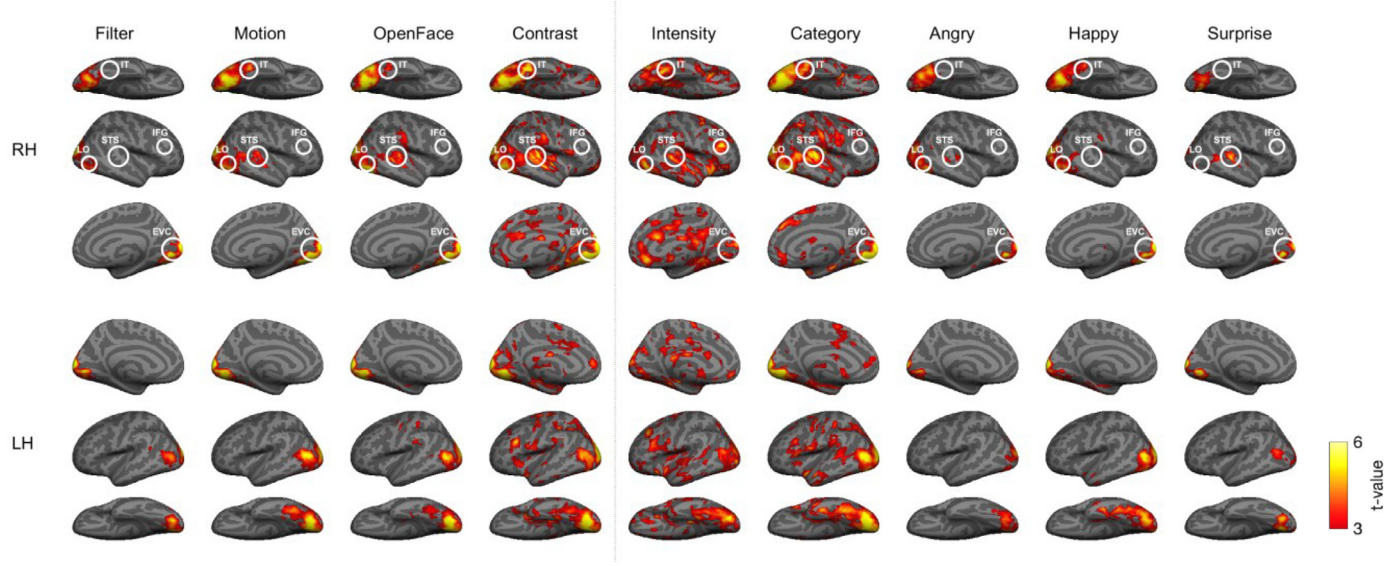

Fig. 2. Significant correlations (permutation test, voxel-wise threshold t=3, cluster-size inference, p<.05) in fMRI for four image-based (left) and five behavioral (right) models. White circles show the approximate location of the most relevant face processing areas, where EVC = early visual cortex; LO = lateral occipital; STS = superior temporal sulcus; IT = inferior temporal; IFG = inferior frontal gyrus.

Table 1
Correlation of behavioral ratings and image morph-levels.

		Behavioral rating			
		Intensity	Angry	Happy	Surprise
Image morphing	Intensity	0.68	-0.10	-0.06	0.08
	Angry	-0.06	0.77	-0.01	-0.10
	Happy	-0.09	0.03	0.72	-0.05
	Surprise	-0.05	-0.08	-0.09	0.68

As seen from the highest values on the diagonal, the behavioral models always correlated most with the respective morph model, as expected.

3.2. FMRI-model correlations

We correlated different models and the fMRI data with the RSA to look for the neural representations of facial expressions in different areas of the brain (Fig. 2). As shown in Fig. 2, many of the models correlated with quite similar areas. For the *image-based* models (*Filter, OpenFace, Motion* and *Contrast*), all of them correlated with the activity patterns in the EVC, the right LO and around the left MT. The *Filter* model did not correlate significantly with any other region. The *OpenFace* model also correlated with the right STS and the right IT, the *Motion* model correlations showed all the same areas and the left IT, while the *Contrast* model correlated with all the same areas as well as several widespread clusters, such as the left IFG. For the *behavioural* models (*Intensity, Category, Angry, Happy, Surprised*), there was more variation. The *Intensity* model correlated with all of the main face areas, including the IT, the right LO, the right STS, and the right IFG. The *Category* model was significant in all of the face processing areas except the right IFG, as well as in the EVC. The *Angry* model only correlated with the EVC and the posterior IT; the *Happy* model with the EVC, the IT, and the left MT/LO; and the *Surprised* model with the EVC and the right STS. Furthermore, especially for the *Intensity, Category* and *Contrast* models, we found sparse and widespread correlations around the brain (Fig. 2). Comparisons with the (lower-bound) noise ceiling (average correlation of each single-subject RDMs to the mean RDM of all the other subjects) showed that none of the model correlations reached the lower noise ceiling level. The maximum model correlation varied from 0.04 to 0.25 between different models, but the maximum of the noise ceiling was 0.32 (see Supplementary Material for full brain image of noise ceiling).

To test the independent role of each of the models, we used partial correlations, controlling for all of the other models (Fig. 3). The models included here were *Filter, OpenFace, Motion, Category* and *Intensity*. For the *Filter* and *Motion* models, this resulted in significant correlations only in the EVC. No significant clusters for the *OpenFace* model were found. The expression *Category* model correlated with the activity patterns in the LO, the IT, and the rSTS, and scattered correlations were found among several areas, including the left anterior STS and the right premotor eye field (area 6v2). Finally, the model for the expression *Intensity* correlated with the IFG, the rSTS, in small clusters in the IT, the right anterior ventral insular (AVI), the right TPOJ, the anterior cingulate cortex, and with several widely dispersed areas around the cortex. To test the robustness of the partial correlation results, we ran partial correlations with all of the different combinations of models that a) always included the intensity and category model, and b) included one, two, three or four of the image-based models. We excluded the single expression models here as the category model is directly created from them. The results from these were remarkably similar to the selected partial model combination.

3.3. EEG-model correlations

The correlations with the models and the EEG data are shown in Fig. 4. The *Category* model correlated significantly with the data, starting around 150 ms after stimulus onset. The correlation reached or was above the lower noise ceiling, suggesting that the model captured the data well. The *Intensity* model, however, did not correlate significantly with EEG at any timepoint. The correlation of the EEG data and the four image-based models (*Motion, Filter, Openface, Contrast*) all showed quite similar time courses, mainly the amplitude of correlation varied, *Motion* model reaching the highest and the *Contrast* model the lowest correlation. *Motion* and *Filter* model correlations showed an early peak and reached significance a bit earlier (around 150 ms) than *OpenFace* and *Contrast* models (around 240 ms). The models based on expression ratings correlated differently with the data. The *Happy* model correlated significantly with the data already starting at 150 ms and the *Angry* model at two separate time windows (350-500 ms and 750-1150 ms). The *Surprise* model did not correlate with the data at any timepoint. In multiple models, the highest correlation peak was around 400 ms (or 160 ms after the video reached full contrast). Overall, the correlation profiles for *Category, Motion* and *Happy* models were highly similar.

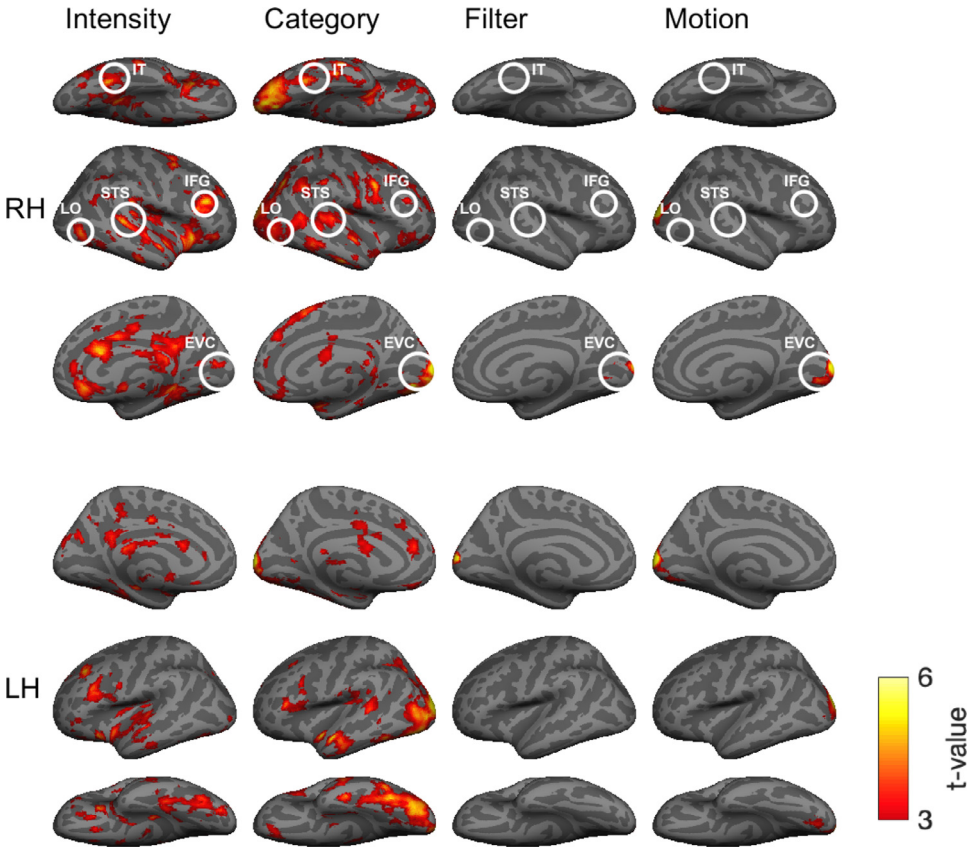

Fig. 3. Partial correlations (permutation test, voxel-wise threshold t=3, cluster-size inference, p<.05) for intensity, category, filter and motion models (no significant correlations were found for the OpenFace model). EVC = early visual cortex; LO = lateral occipital; STS = superior temporal sulcus; IT = inferior temporal; IFG = inferior frontal gyrus.

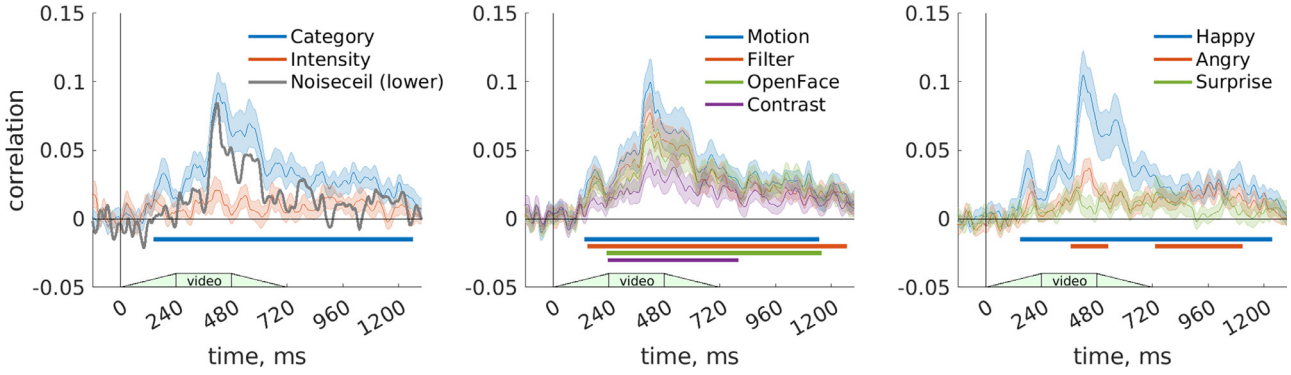

Fig. 4. EEG-model correlations. Straight lines show significant timings for each model (permutation test, cluster-weight inference, p<.05). On left, the lower-bound of the noise ceiling is plotted with a grey line.

For partial correlations (Fig. 5), the *Category* model remained significant between 360 and 620 ms, and the *Motion* model between 240 and 620 ms, while *Filter* and *OpenFace* were no longer significant. The *Intensity* model again showed no significant correlations. We conducted the same robustness check as for the fMRI (see above; not shown). The results remained practically the same for all model combinations, specifically in terms of the *Category* and *Motion* models always correlating with the data, *Intensity, OpenFace,* and *Contrast* being insignificant in all combinations, and the *Filter* model showing significant correlations in all combinations where the motion model was excluded, but not in any other combination.

3.4. EEG-fMRI correlations

We correlated each timepoint in the EEG data with each voxel in the fMRI data to create a four-dimensional spatio-temporal map of facial expression processing (Fig. 6). The results show significant correlations starting at around 100 ms from the EVC and ending at around 1150 ms. Parts of the EVC were significant for the whole duration. The first correlations outside the EVC were between 300 and 350 ms in the left MT/LO, and after 400 ms again in the left MT/LO, the right LO, and small patches in the IT. The most widespread correlations were found at 500 ms when the correlations also spread to the right STS and to a large part of the left IT, but not the right IT.

4. Discussion

We studied the spatio-temporal processing of facial expressions in the brain using representational similarity analysis (RSA) in both fMRI and EEG data. We created a stimulus space from short videos of faces varying both in expression intensity and expression category. There were three different expressions (angry, happy, surprised), varying dimensionally from a neutral to a full-blown expression, as well as dimensionally from each expression to the others. We calculated representa-

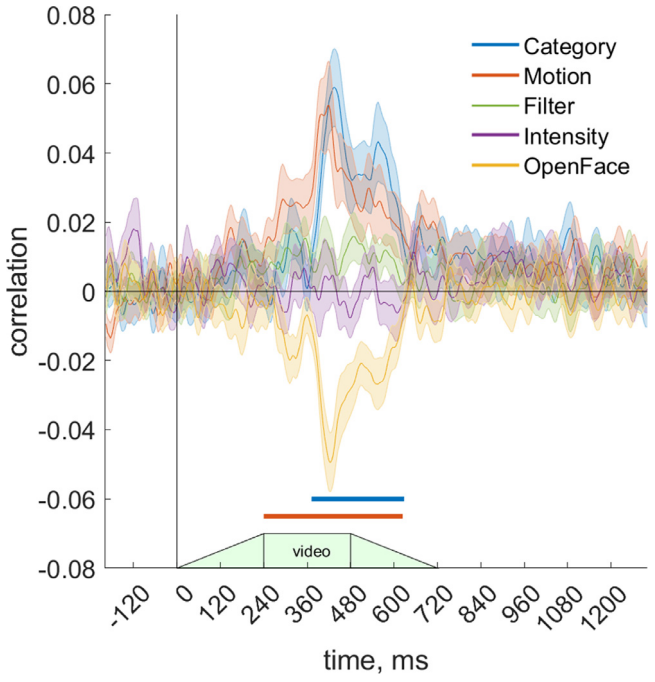

Fig. 5. EEG-model partial correlations. Lines show significant timings for each model (cluster-based permutation analysis).

tional dissimilarity matrices (RDMs) from the neural responses between each possible stimulus pair, and thus had separate RDMs for each voxel (from the fMRI) and timepoint (from the EEG). This allowed us to compare the neural representations of facial expressions in different areas and at different times to each other, as well as to different models derived from either behavioural ratings of the videos, or image properties in the videos. Our results in the fMRI showed that, when accounting for low-level features, the IFG-FA processes only the intensity of expressions, while the LO, the STS and the IT face areas code both expression intensity and expression category. The EEG data correlated with the fMRI starting at 100 ms in the EVC, spreading to the LO, the IT, and the STS at around 400–500 ms, as well as with the model of expression category and image-based models especially around 400 ms, with no correlation with the intensity model. Our results reveal the distinct role of IFG-FA coding intensity of expression, while other known face areas contained information both on the expression category and intensity.

Faces provide a platform for the study of changing representations of information in the brain. As subtle visual changes in a face can signal the difference between a loved one and a stranger, or an angry and a happy person, the efficient transformation of those visual features into these higher-level qualities must occur somewhere, at some time in our brain. Solving the spatiotemporal pattern of these transformations might thus provide important insights into the wider question of how our brain processes sensory information into a behaviourally usable form. By using facial expressions, we created a stimulus space where, for example, the perceived angriness and emotional intensity of faces varied dimensionally and, importantly, we could separate the low-level image-based changes and motion from changes in perceived intensity. In addition, the use of multivariate pattern analysis (MVPA) and RSA allowed us to look into the more finely knitted structure of information in different brain regions and at different times. Hence, while several studies have looked into the processing of facial expressions in the brain, very few have used a stimulus space as a variable, as in our study, which allowed us to explicitly separate and compare models of expression category, expression intensity and image-based features (see also our earlier study, Muukkonen et al., 2020).

In the fMRI, our results show that, when controlling for low-level features, the IFG codes the intensity of expression. The other known main face areas, namely the LO, IT (containing the FFA) and STS, contained information about both the intensity and the category of expressions. The clusters found for intensity and category in these regions were, however, quite dissimilar, with partly separate spatial locations in the STS and a larger cluster for category than intensity in the left IT. Previous studies have shown that the IFG-FA, as well as the STS, are particularly sensitive to dynamic faces (e.g., Fox et al., 2009; Furl et al., 2010; Pitcher, Dilks, et al., 2011; Pitcher et al., 2014; Yoshikawa & Sato, 2006). This might explain the difference in terms of the current study finding responses in these areas, while our previous similar study using static facial expressions did not (Muukkonen et al., 2020). We found that while the STS correlated with multiple models, the IFG-FA coded only the expression intensity, thus suggesting a change in the neural representations in the dorsal face path, with the IFG-FA showing more abstract processing of expression intensity. Previous studies have found higher responses in the IFG-FA to asynchronous than synchronous movements of the eyes and mouth (Skiba & Vuilleumier, 2020), and more holistic representation of eyes and mouth in the IFG-FA than in the STS (Flack et al., 2015). Nor did Skiba and Vuilleumier (2020) find emotion intensity coding in the IFG-FA, only in the STS, although their study contained less intensity variation, while the current study was specifically designed to reveal the processing of expression intensity. While our stimuli set was different compared to those studies and did not allow for testing the in-

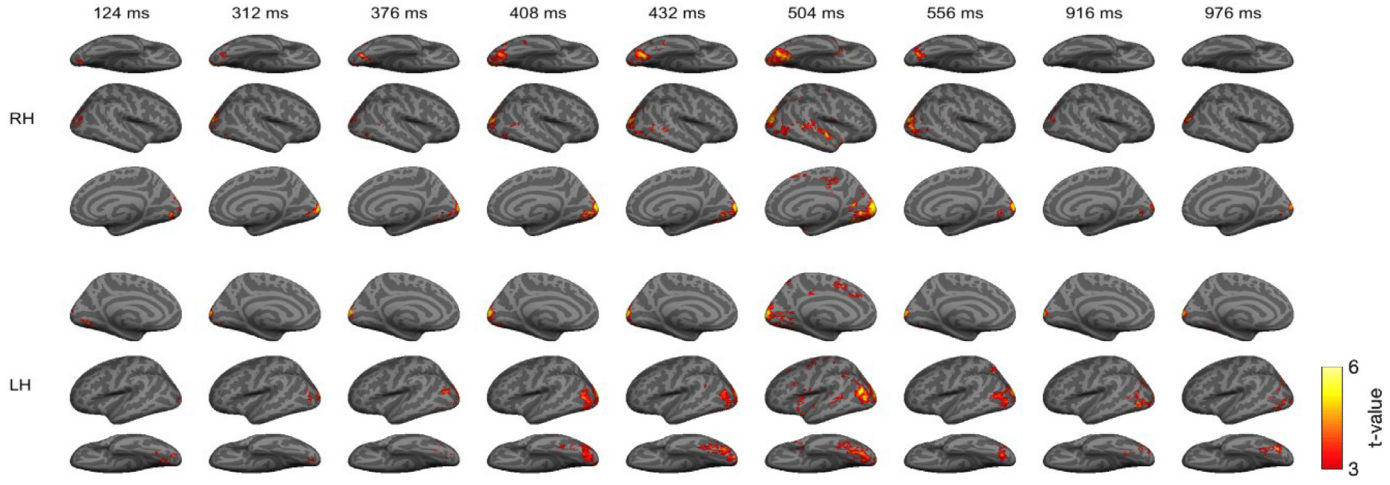

Fig. 6. EEG-fMRI correlations at selected timepoints.

tegration of face parts, our results support the wider suggestion of more abstract, higher-level coding of expressive faces in the IFG-FA than in the STS.

Furthermore, we found several other areas coding the expression intensity and category, such as the right anterior ventral insular (AVI), the cingulate cortex, and the ventral premotor cortex (area 6v2). While not considered part of the main face processing network (Duchaine & Yovel, 2015), similar areas have been found in functional connectivity analysis for face processing (Zhen, Fang, & Liu, 2013), particularly showing that the AVI and cingulate cortex were part of the expression processing network. For the premotor area, at least a single study has found this same area when contrasting dynamic and static facial expressions (Sato, Kochiyama, Yoshikawa, Naito, & Matsumura, 2004). Thus, while the evidence for the role of these areas in facial expression processing is sparse, our study suggests that they have a role in more abstract expression processing, and stresses the usefulness of using the spatially unbiased searchlight analysis. In addition, when not controlling for other models, we found the whole-face processing network (IFG withstanding) to correlate with the variation in the mean contrast of the faces. As the variation in contrast in our stimuli was minimal, this was a rather surprising result. However, these correlations did not stand after controlling for other models, suggesting that these areas did not code contrast per se. As the contrast variation model has rarely been included in studies of the neural processing of faces, our results encourage future studies to test this rather simple model as well.

The EEG and fMRI correlations for individual expression models were quite different. The *Happy* model correlated with EEG for a long time period, the *Angry* model in a two separate time windows, and the *Surprised* model did not reveal any significant correlations. The higher correlation with the *Happy* model in comparison to *Angry* and *Surprised* models is consistent with behavioral ratings that showed also highest reliability for happy ratings. In fMRI, the *Category* model revealed much more widespread correlations than the individual expression models. Since the *Category* model was constructed on the basis of *Angry, Happy* and *Surprised* models, the more widespread correlations suggest that many face areas process differences between expressions rather than expressions per se. In EEG, the correlation profile of the *Happy* model was quite similar with the *Motion/Filter* models, showing the strong association of happy expression and low-level image features.

On the temporal processing of facial expressions in the brain, our results showed that low-level features as well as the expression category and happiness already correlated with the EEG data at around 150 ms, and peaked at 400 ms, consistent with previous study applying multivariate methods on EEG (Smith & Smith, 2019). While showing widespread correlations in the fMRI, there was no indication of expression-intensity coding in the EEG, consistent with our previous study (Muukkonen et al., 2020) but in contrast with some previous studies finding intensity coding in the EEG (Leleu et al., 2018; Recio et al., 2014; Sprengelmeyer & Jentzsch, 2006). When controlling for other models, we found motion coding starting at around 240 ms, and category processing at around 360 ms, while no other models remained significant. It should be noted, however, that our different models showed very similar correlation structures, all peaking at the same time, and thus not revealing any clear processing steps, for example from low-level features to more abstract features. The use of video clips instead of still images makes the timings harder to interpret, as the fast processing of the later frames might co-occur with the later processing steps of the earlier frames. This is evident in the filter model correlations, which, unlike in previous studies (Dima et al., 2018; Muukkonen et al., 2020), did not rapidly show the highest peak at around 100 ms, but only later at 400 ms. However, stronger, earlier or more widespread activity has been typically reported when comparing dynamic faces to static faces or dynamic control stimuli (e.g., Furl et al., 2010; Puce et al., 2003; Recio et al., 2011; Sato et al., 2015; Trautmann-Lengsfeld et al., 2013). Thus, another possibility is that the linear contrast fade in that we used, might have disrupted the EEG signal so that the processing of face onset, the initial expression of the face and the later change in expression all overlap.

The EEG-fMRI correlations showed the EEG to correlate only with the EVC until 300 ms, when the EEG correlated with the left MT/LO. Around 400 ms, and especially at 500 ms, more widespread correlations were found in the IT, the LO, and the STS. Thus, these peaks matched the timing of the highest EEG-model correlations, and showed the same areas as the fMRI-model correlations for the models with the highest correlations in the EEG-model analysis (namely, category and motion models). Consistently with the null findings for intensity coding in the EEG, we found no EEG-fMRI correlations in the IFG, which was found to code intensity in the fMRI analysis. The order of the EEG-fMRI correlations from EVC to LO to IT/STS was similar to our previous study (Muukkonen et al., 2020), while the absolute timings were considerably delayed. We assume that this was due to the use of video clips and/or the contrast fade in and their effect in the EEG data. Interestingly, as in the aforementioned previous study, we again found significant EEG-fMRI correlations, mainly in the left IT and not the right, despite the right-pronounced lateralization of face processing.

With regard to the limitations of our study, we first note the different results from the cross-validated measures (crossnobis, SVM) and the reported correlation results, especially in the fMRI (see Supplementary Material). While the reason for this remains unclear, some possible explanations include the small number of trials (2) per stimuli in a single run, the randomly varying identity of the face, the use of two different tasks varying between runs, having measurements from two separate sessions, and having a long resting period in the middle of the run instead of null trials. Furthermore, the effect of mean-pattern normalization on the results was substantial, unsurprisingly as mean-pattern normalization can change the RDM pattern dramatically (Walther et al., 2016). It is possible that this reflects some property of the neural code, although the effect of MPR will vary depending on the used stimulus space, which makes it harder to interpret, while the use of stimuli that contain more variation than in our study might cause different effects. Next, while dynamic stimuli elicit higher responses in the dorsal face path in the fMRI, for the EEG results, the use of videos instead of still images makes our results hard to compare to previous studies, although a previous study did find a similar EEG structure with short video clips as with static images (Recio et al., 2014). As the video progresses in time, we cannot clearly state whether, for example, the peak at 400 ms after video onset is comparable to results in other studies at 400 ms, as it might also relate to some faster processing of later frames in the video. Furthermore, our stimuli differ from previous studies in that our videos started with a gradual contrast fade in. In addition, our stimulus set was specifically designed to study the effect of expression intensity and to separate it from the low-level image-based features and motion. In contrast, the models for categorical expressions correlated highly with the low-level model, and thus showed less difference from low-level features. Finally, we used a model for contrast differences in the stimuli, even though the changes in contrast between the stimuli were minimal and should probably not have any effect per se. Nevertheless, the contrast model had very strong correlations with the face processing network (when other models were not controlled for), and thus might also capture some property of the neural code of face processing.

To sum up, we used a novel, dimensionally varying and dynamic stimulus set to study the temporal and spatial processing of facial expression intensities and categories. Our fMRI results suggest that the IFG codes the intensity of facial expression, and the LO, the IT and the STS code both of these features. For the timings of these processes, our EEG results showed significant coding in particular of low-level features, expression category and happiness from 150 ms until 1200 ms, especially around 400 ms. Correspondingly, the EEG-fMRI analysis showed correlations starting after 100 ms in the EVC, spreading to the left MT/LO at 300 ms, and being most widespread at 400–500 ms, including the LO, especially the left IT, and the right STS. Our results show representational transformation from lower-level processing of visual features

in posterior face areas to coding of abstract expression intensity in the IFG-FA.

Data and code availability statements

The data are not openly available due to restrictions imposed by the local ethics committee. All preprocessed data (but not raw images) are available upon request. A data-sharing agreement is needed for sharing preprocessed data. All analysis codes are available upon request with no restrictions.

Data availability

Data will be made available on request.

Credit authorship contribution statement

I. Muukkonen: Conceptualization, Methodology, Software, Formal analysis, Investigation, Writing – original draft, Writing – review & editing, Visualization. **V.R. Salmela:** Conceptualization, Methodology, Software, Investigation, Writing – review & editing, Visualization, Supervision, Funding acquisition.

Acknowledgements

This work was supported by an Academy of Finland grant to VRS (grant number 298329).

Supplementary materials

Supplementary material associated with this article can be found, in the online version, at doi:10.1016/j.neuroimage.2022.119631.

References

Amos, B, Ludwiczuk, B, Satyanarayanan, M, 2016. Openface: A general-purpose face recognition library with mobile applications. *CMU School of Computer Science*, 6(2). Retrieved from http://reports-archive.adm.cs.cmu.edu/anon/anon/usr0/ftp/2016/CMU-CS-16-118.pdf.

Anzellotti, S, Caramazza, A, 2016. From parts to identity: invariance and sensitivity of face representations to different face halves. Cereb. Cortex 26 (5), 1900–1909. doi:10.1093/cercor/bhu337.

Anzellotti, S, Fairhall, SL, Caramazza, A, 2014. Decoding representations of face identity that are tolerant to rotation. Cereb. Cortex 24 (8), 1988–1995. doi:10.1093/cercor/bht046.

Atkinson, AP, Adolphs, R, 2011. The neuropsychology of face perception: beyond simple dissociations and functional selectivity. Philos. Trans. Royal Soci. London. Series B, Biol. Sci. 366 (1571), 1726–1738. doi:10.1098/rstb.2010.0349.

Bernstein, M, Yovel, G, 2015. Two neural pathways of face processing: a critical evaluation of current models. Neurosci. Biobehav. Rev. 55, 536–546. doi:10.1016/j.neubiorev.2015.06.010.

Carlin, JD, Kriegeskorte, N, 2017. Adjudicating between face-coding models with individual-face fMRI responses. PLoS Comput. Biol. 13 (7), 1–28. doi:10.1371/journal.pcbi.1005604.

Chan, AWY, Downing, PE, 2011. Faces and eyes in human lateral prefrontal cortex. Front. Human Neurosci. 5 (JUNE), 1–10. doi:10.3389/fnhum.2011.00051.

Chang, L, Tsao, DY, 2017. The code for facial identity in the primate brain. Cell 169 (6), 1013–1020. doi:10.1016/j.cell.2017.05.011, e14.

Collins, JA, Olson, IR, 2015. Beyond the FFA: the role of the ventral anterior temporal lobes in face processing. Neuropsychologia 65–79. doi:10.1016/j.neuropsychologia.2014.06.005.

Deen, B, Saxe, R, 2019. Parts-based representations of perceived face movements in the superior temporal sulcus. Hum. Brain Mapp. 40 (8), 2499–2510. doi:10.1002/hbm.24540.

Dima, DC, Perry, G, Messaritaki, E, Zhang, J, Singh, KD, 2018. Spatiotemporal dynamics in human visual cortex rapidly encode the emotional content of faces. Hum. Brain Mapp. doi:10.1002/hbm.24226.

Dobs, K, Isik, L, Pantazis, D, Kanwisher, N, 2019. How face perception unfolds over time. Nat. Commun. 10 (1), 1258. doi:10.1038/s41467-019-09239-1.

Dobs, K, Schultz, J, Bülthoff, I, Gardner, JL, 2018. Task-dependent enhancement of facial expression and identity representations in human cortex. Neuroimage 172 (July 2017), 689–702. doi:10.1016/j.neuroimage.2018.02.013.

Duchaine, B, Yovel, G, 2015. A Revised Neural Framework for Face Processing. Ann. Rev. Vision Sci. 1 (1), 393–416. doi:10.1146/annurev-vision-082114-035518.

Dzhelyova, M, Jacques, C, Rossion, B, 2017. At a single glance: Fast periodic visual stimulation uncovers the spatio-temporal dynamics of brief facial expression changes in the human brain. Cereb. Cortex 27 (8), 4106–4123. doi:10.1093/cercor/bhw223.

Eifuku, S, 2014. Neural representations of perceptual and semantic identities of individuals in the anterior ventral inferior temporal cortex of monkeys. Japanese Psychol. Res. 56 (1), 58–75. doi:10.1111/jpr.12026.

Engell, AD, Haxby, JV, 2007. Facial expression and gaze-direction in human superior temporal sulcus. Neuropsychologia 45 (14), 3234–3241. doi:10.1016/j.neuropsychologia.2007.06.022.

Esteban, O, Blair, RW, Markiewicz, CJ, Berleant, SL, Moodie, G, Ma, F, Isik, AI et al. (2018). "FMRIPrep." Software. Zenodo. 10.5281/zenodo.852659.

Esteban, O, Markiewicz, CJ, Blair, RW, Moodie, GA, Isik, AI, Erramuzpe, A, Kent, J, et al., 2018. fMRIPrep: a robust preprocessing pipeline for functional MRI. Nat. Methods doi:10.1038/s41592-018-0235-4.

Flack, TR, Andrews, TJ, Hymers, M, Al-Mosaiwi, M, Marsden, SP, Strachan, JWA, … Young, AW, 2015. Responses in the right posterior superior temporal sulcus show a feature-based response to facial expression. Cortex 69, 14–23. doi:10.1016/j.cortex.2015.03.002.

Foley, E, Rippon, G, Thai, NJ, Longe, O, Senior, C, 2012. Dynamic facial expressions evoke distinct activation in the face perception network: a connectivity analysis study. J. Cogn. Neurosci. 24 (2), 507–520. doi:10.1162/jocn_a_00120.

Fox, CJ, Moon, SY, Iaria, G, Barton, JJS, 2009. The correlates of subjective perception of identity and expression in the face network: an fMRI adaptation study. Neuroimage 44 (2), 569–580. doi:10.1016/j.neuroimage.2008.09.011.

Freiwald, WA, Tsao, DY, 2010. Functional compartmentalization and viewpoint generalization within the macaque face-processing system. Science 330 (5), 845–851. doi:10.1126/science.1229223.

Freiwald, WA, Tsao, DY, Livingstone, MS, 2009. A face feature space in the macaque temporal lobe. Nat. Neurosci. 12 (9), 1187–1196. doi:10.1038/nn.2363.

Furl, N, van Rijsbergen, NJ, Kiebel, SJ, Friston, KJ, Treves, A, Dolan, RJ, 2010. Modulation of perception and brain activity by predictable trajectories of facial expressions. Cereb Cortex 20 (3), 694–703. doi:10.1093/cercor/bhp140.

Greening, SG, Mitchell, DGV, Smith, FW, 2018. Spatially generalizable representations of facial expressions: decoding across partial face samples. Cortex 101, 31–43. doi:10.1016/j.cortex.2017.11.016.

Harris, RJ, Young, AW, Andrews, TJ, 2012. Morphing between expressions dissociates continuous from categorical representations of facial expression in the human brain. Proc. Nat. Acad. Sci. U.S.A. 109 (51), 21164–21169. doi:10.1073/pnas.1212207110.

Harris, RJ, Young, AW, Andrews, TJ, 2014. Dynamic stimuli demonstrate a categorical representation of facial expression in the amygdala. Neuropsychologia 56 (1), 47–52. doi:10.1016/j.neuropsychologia.2014.01.005.

Henriksson, L, Mur, M, Kriegeskorte, N, 2015. Faciotopy – A face-feature map with face-like topology in the human occipital face area. Cortex 72, 156–167. doi:10.1016/j.cortex.2015.06.030.

Hinojosa, JA, Mercado, F, Carretié, L, 2015. N170 sensitivity to facial expression: a meta-analysis. Neurosci. Biobehav. Rev. 55, 498–509. doi:10.1016/J.NEUBIOREV.2015.06.002.

Hyvärinen, A, 1999. Fast and robust fixed-point algorithms for independent component analysis. IEEE Trans. Neural Networks 10 (3), 626–634. Retrieved from http://ieeexplore.ieee.org/stamp/stamp.jsp?tp=&arnumber=761722%5Cnpapers3://publication/doi/10.1109/72.761722 .

Kanwisher, N, 2000. Domain specificity in face perception. Nat. Neurosci. 3 (8), 759–763. doi:10.1038/77664.

Kanwisher, N, Yovel, G, 2006. The fusiform face area: a cortical region specialized for the perception of faces. Philos. Trans. Royal Soc. London. Series B, Biol. Sci. 361 (1476), 2109–2128. doi:10.1098/rstb.2006.1934.

Kovács, G, 2020. Getting to know someone: Familiarity, person recognition, and identification in the human brain. J. Cogn. Neurosci. 32 (12), 2205–2225. doi:10.1162/jocn_a_01627.

Kriegeskorte, N, Formisano, E, Sorger, B, Goebel, R, 2007. Individual faces elicit distinct response patterns in human anterior temporal cortex. Proc. Nat. Acad. Sci. U.S.A. 104 (51), 20600–20605. doi:10.1073/pnas.0705654104.

Kriegeskorte, N, Goebel, R, Bandettini, Pa, 2006. Information-based functional brain mapping. Proc. Nat. Acad. Sci. U.S.A. 103 (10), 3863–3868. doi:10.1073/pnas.0600244103.

Kriegeskorte, N, Mur, M, Bandettini, Pa, 2008. Representational similarity analysis – connecting the branches of systems neuroscience. Front. Syst. Neurosci. 2 (November), 4. doi:10.3389/neuro.06.004.2008.

Langner, O, Dotsch, R, Bijlstra, G, Wigboldus, DHJ, Hawk, ST, van Knippenberg, A, 2010. Presentation and validation of the radboud faces database. CognitEmot. 24 (8), 1377–1388. doi:10.1080/02699930903485076.

Leleu, A, Dzhelyova, M, Rossion, B, Brochard, R, Durand, K, Schaal, B, Baudouin, JY, 2018. Tuning functions for automatic detection of brief changes of facial expression in the human brain. Neuroimage 179 (October 2017), 235–251. doi:10.1016/j.neuroimage.2018.06.048.

Leopold, DA, Bondar, IV, Giese, MA, 2006. Norm-based face encoding by single neurons in the monkey inferotemporal cortex. Nature 442 (7102), 572–575. doi:10.1038/nature04951.

Leppänen, JM, Kauppinen, P, Peltola, MJ, Hietanen, JK, 2007. Differential electrocortical responses to increasing intensities of fearful and happy emotional expressions. Brain Res. 1166 (1), 103–109. doi:10.1016/j.brainres.2007.06.060.

Mognon, A, Jovicich, J, Bruzzone, L, Buiatti, M, 2011. ADJUST: An automatic EEG artifact detector based on the joint use of spatial and temporal features. Psychophysiology 48 (2), 229–240. doi:10.1111/j.1469-8986.2010.01061.x.

Müller-Bardorff, M, Bruchmann, M, Mothes-Lasch, M, Zwitserlood, P, Schlossmacher, I, Hofmann, D, … Straube, T, 2018. Early brain responses to af-

fective faces: a simultaneous EEG-fMRI study. Neuroimage 178, 660–667. doi:10.1016/J.NEUROIMAGE.2018.05.081.
Muukkonen, I, Ölander, K, Numminen, J, Salmela, VR, 2020. Spatio-temporal dynamics of face perception. Neuroimage 209. doi:10.1016/j.neuroimage.2020.116531.
Nichols, TE, Holmes, AP, 2001. Nonparametric permutation tests for functional neuroimaging: a primer with examples. Hum. Brain Mapp. 15, 1–25. doi:10.1002/hbm.1058.
Perrett, DI, Rolls, ET, Caan, W, 1982. Visual neurones responsive to faces in the monkey temporal cortex. Exp. Brain Res. 47 (47), 329–342.
Pitcher, D, Dilks, DD, Saxe, RR, Triantafyllou, C, Kanwisher, N, 2011. Differential selectivity for dynamic versus static information in face-selective cortical regions. Neuroimage 56 (4), 2356–2363. doi:10.1016/j.neuroimage.2011.03.067.
Pitcher, D, Duchaine, B, Walsh, V, 2014. Combined TMS and fMRI reveal dissociable cortical pathways for dynamic and static face perception. Curr. Biol. 24 (17), 2066–2070. doi:10.1016/j.cub.2014.07.060.
Pitcher, D, Walsh, V, Duchaine, B, 2011. The role of the occipital face area in the cortical face perception network. Exp. Brain Res. 209 (4), 481–493. doi:10.1007/s00221-011-2579-1.
Poncet, F, Baudouin, JY, Dzhelyova, MP, Rossion, B, Leleu, A, 2019. Rapid and automatic discrimination between facial expressions in the human brain. Neuropsychologia 129 (February), 47–55. doi:10.1016/j.neuropsychologia.2019.03.006.
Puce, A, Smith, A, Allison, T, 2000. Erps evoked by viewing facial movements. Cogn Neuropsychol 17 (1), 221–239. doi:10.1080/026432900380580.
Puce, A, Syngeniotis, A, Thompson, JC, Abbott, DF, Wheaton, KJ, Castiello, U, 2003. The human temporal lobe integrates facial form and motion: evidence from fMRI and ERP studies. Neuroimage 19 (3), 861–869. doi:10.1016/s1053-8119(03)00189-7.
Recio, G, Schacht, A, Sommer, W, 2014. Recognizing dynamic facial expressions of emotion: specificity and intensity effects in event-related brain potentials. Biol. Psychol. 96 (1), 111–125. doi:10.1016/j.biopsycho.2013.12.003.
Recio, G, Sommer, W, Schacht, A, 2011. Electrophysiological correlates of perceiving and evaluating static and dynamic facial emotional expressions. Brain Res. 1376, 66–75. doi:10.1016/j.brainres.2010.12.041.
Ritchie, JB, Lee Masson, H, Bracci, S, Op de Beeck, HP, 2021. The unreliable influence of multivariate noise normalization on the reliability of neural dissimilarity. Neuroimage 245 (October), 118686. doi:10.1016/j.neuroimage.2021.118686.
Rossion, B, 2018. Humans are visual experts at unfamiliar face recognition. Trends Cogn. Sci. 22 (6), 471–472. doi:10.1016/j.tics.2018.03.002.
Rossion, B, Jacques, C, 2011. The N170: understanding the time-course of face perception in the human brain. Oxford Handbook ERP Components 115–142. doi:10.1093/oxfordhb/9780195374148.013.0064, December.
Said, CP, Haxby, JV, Todorov, A, 2011. Brain systems for assessing the affective value of faces. Philos. Trans. Royal Soc. London B 366 (1571), 1660–1670. doi:10.1098/rstb.2010.0351.
Sato, W, Kochiyama, T, Uono, S, 2015. Spatiotemporal neural network dynamics for the processing of dynamic facial expressions. Sci. Rep. 5, 12432. doi:10.1038/srep12432.
Sato, W, Kochiyama, T, Yoshikawa, S, Naito, E, Matsumura, M, 2004. Enhanced neural activity in response to dynamic facial expressions of emotion: An fMRI study. Cognit. Brain Res. 20 (1), 81–91. doi:10.1016/j.cogbrainres.2004.01.008.
Skiba, RM, Vuilleumier, P, 2020. Brain networks processing temporal information in dynamic facial expressions. Cereb. Cortex 30 (11), 6021–6038. doi:10.1093/cercor/bhaa176.
Smith, FW, Smith, ML, 2019. Decoding the dynamic representation of facial expressions of emotion in explicit and incidental tasks. Neuroimage 195, 261–271. doi:10.1016/j.neuroimage.2019.03.065.
Sormaz, M, Watson, DM, Smith, WAP, Young, AW, Andrews, TJ, 2016. Modelling the perceptual similarity of facial expressions from image statistics and neural responses. Neuroimage 129, 64–71. doi:10.1016/j.neuroimage.2016.01.041.
Sprengelmeyer, R, Jentzsch, I, 2006. Event related potentials and the perception of intensity in facial expressions. Neuropsychologia 44 (14), 2899–2906. doi:10.1016/j.neuropsychologia.2006.06.020.
Srinivasan, R, Golomb, JD, Martinez, AM, 2016. A neural basis of facial action recognition in humans. J. Neurosci. 36 (16), 4434–4442. doi:10.1523/JNEUROSCI.1704-15.2016.
Sugase, Y, Yamane, S, Ueno, S, Kawano, K, 1999. Global and fine information coded by single neurons in the temporal visual cortex. Nature 400 (6747), 869–873. doi:10.1038/23703.
Trautmann-Lengsfeld, SA, Dominguez-Borras, J, Escera, C, Herrmann, M, Fehr, T, 2013. The perception of dynamic and static facial expressions of happiness and disgust investigated by ERPs and fMRI constrained source analysis. PLoS One 8 (6), e66997. doi:10.1371/journal.pone.0066997.
Trautmann, SA, Fehr, T, Herrmann, M, 2009. Emotions in motion: dynamic compared to static facial expressions of disgust and happiness reveal more widespread emotion-specific activations. Brain Res. 1284, 100–115. doi:10.1016/j.brainres.2009.05.075.
Walther, A, Nili, H, Ejaz, N, Alink, A, Kriegeskorte, N, Diedrichsen, J, 2016. Reliability of dissimilarity measures for multi-voxel pattern analysis. Neuroimage 137, 188–200. doi:10.1016/j.neuroimage.2015.12.012.
Watanabe, S, Kakigi, R, Puce, A, 2001. Occipitotemporal activity elicited by viewing eye movements: a magnetoencephalographic study. Neuroimage 13 (2), 351–363. doi:10.1006/nimg.2000.0682.
Watson, R, Latinus, M, Noguchi, T, Garrod, O, Crabbe, F, Belin, P, 2014. Crossmodal adaptation in right posterior superior temporal sulcus during face–voice emotional integration. J. Neurosci. 34 (20), 6813–6821. doi:10.1523/JNEUROSCI.4478-13.2014.
Winston, JS, O'Doherty, J, Dolan, RJ, 2003. Common and distinct neural responses during direct and incidental processing of multiple facial emotions. Neuroimage 20 (1), 84–97. doi:10.1016/S1053-8119(03)00303-3.
Yang, Z, Freiwald, WA, 2021. Joint encoding of facial identity, orientation, gaze, and expression in the middle dorsal face area. Proc. Natl. Acad. Sci. 118 (33), e2108283118. doi:10.1073/pnas.2108283118.
Yoshikawa, S, Sato, W, 2006. Enhanced perceptual, emotional, and motor processing in response to dynamic facial expressions of emotion. Japanese Psychol. Res. 48 (3), 213–222. doi:10.1111/j.1468-5884.2006.00321.x.
Zhang, H, Japee, S, Nolan, R, Chu, C, Liu, N, Ungerleider, LG, 2016. Face-selective regions differ in their ability to classify facial expressions. Neuroimage 130, 77–90. doi:10.1016/j.neuroimage.2016.01.045.
Zhen, Z, Fang, H, Liu, J, 2013. The Hierarchical Brain Network for Face Recognition. PLoS One 8 (3), e59886. doi:10.1371/journal.pone.0059886.